Supplementary Material

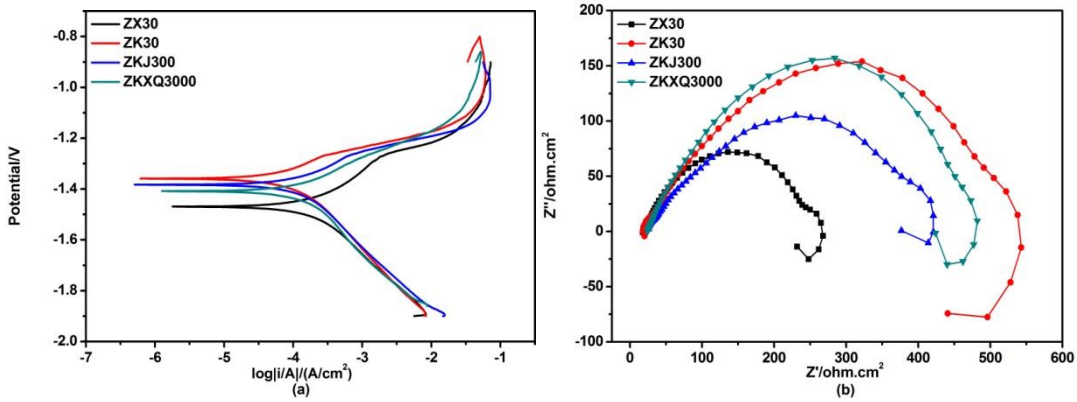

Fig.S1. The polarization curve (**a**) and alternating current (AC) impedance spectra (**b**) of ZX30, ZK30, ZKJ300 and ZKXQ3000 alloys

Electrochemical experiments were carried out using Zahner electrochemical workstation (Zennium, Germany) in simulated body fluid at room temperature. A three-electrode cell assembly consists with magnesium alloys as the working electrode, graphite as an auxiliary electrode and saturated calomel as a reference electrode respectively. Prior to electrochemical impedance spectroscopy (EIS) and polarization testing, all the samples were allowed to stabilize for a period of 3600 s to attain open circuit potential (OCP). EIS was performed after stabilization at OCP within the frequency range of 100 KHz - 0.1 Hz. Dynamic polarization experiments were conducted at a scan rate of 1 mV/s. Experiments were repeated for thrice to attain the accuracy and stability during the measurements.

Figure S1(a) presents the potentiodynamic polarization curves of ZX30, ZK30, ZKJ300 and ZKXQ3000 alloys. It can be seen that the ZK30 alloy shows a positive shift in the corrosion potential, indicating that the addition of Zr reduced the driving force for corrosion. In addition, the ZXJ300 alloy had a relatively high current density during cathodic polarization, so that the hydrogen evolution reaction on the surface of the ZXJ300 was relatively intense. In the anodic polarization process, the current density of the ZX30 alloy electrode was bigger at the same potential, having a larger growth rate with potential ennobled, manifesting that the addition of Ca made the anode dissolution relatively faster. It can be concluded that the corrosion current densities of ZX30, ZK30, ZKJ300, and ZKXQ3000 alloys were 107.4 μA/cm^2, 44.8 μA/cm^2, 85.8 μA/cm^2, and 80.2 μA/cm^2 respectively according to the polarization curve using Tafel extrapolation, showing ZK30 had good corrosion resistance.

Figure 5(b) shows the AC impedance spectra of ZX30, ZK30, ZKJ300, and ZKXQ3000 alloys. All the magnesium alloys showed two capacitive loops in the high and middle frequency regions and an inductive loop in the low frequency region. The high-frequency and intermediate-frequency capacitive loops were related to charge transfer resistance and the magnesium hydroxide film covering on the electrode surface[1]. The larger capacitive loop turned out that the charge transfer was inhibited strongly[2]. The inductive loop in the low frequency region characterized the diffusion rate of the reactants or products of the electrode reaction, when the diffusion rate was slower, then larger, the inductive loop existed. Obviously, the ZK30 alloy had the largest capacitance loop in the high frequency and intermediate frequency regions, which indicated the electrochemical process of the ZK30 alloy was the slowest.

It is known that the corrosion resistance of ZK30 is optimal among the four alloys from the polarization curve and AC impedance spectra. This is because the electrochemical behavior of magnesium alloys is not only related to the composition of the magnesium alloy but also related to the content and distribution of the second phase in the magnesium alloy. The second-phase precipitated phases are often nobler than the magnesium matrix, which could lead to micro-galvanic corrosion acceleration and finally induce local corrosion damage [3,4]. It can be observed

from Fig. 1 that all other three magnesium alloys except ZK30 have more second phases distributed around the grain boundaries, which means fewer corrosion sites and uniform attack can be produced in the ZK30 alloy.

References

1. Zhao, M.-C.; Schmutz, P.; Brunner, S.; Liu, M.; Song, G.-l.; Atrens, A. An exploratory study of the corrosion of Mg alloys during interrupted salt spray testing. Corrosion Science 2009, 51, 1277-1292, DOI: 10.1016/j.corsci.2009.03.014.
2. Oh-ishi, K.; Mendis, C. L.; Homma, T.; Kamado, S.; Ohkubo, T.; Hono, K. Bimodally grained microstructure development during hot extrusion of Mg–2.4 Zn–0.1 Ag–0.1 Ca–0.16 Zr (at.%) alloys. Acta Materialia 2009, 57, 5593-5604, DOI: 10.1016/j.actamat.2009.07.057.
3. Zander, D.; Zumdick, N. A. Influence of Ca and Zn on the microstructure and corrosion of biodegradable Mg–Ca–Zn alloys. Corrosion Science 2015, 93, 222-233, DOI: 10.1016/j.corsci.2015.01.027.
4. Han, P.; Cheng, P.; Zhang, S.; Zhao, C.; Ni, J.; Zhang, Y.; Zhong, W.; Hou, P.; Zhang, X.; Zheng, Y.; Chai, Y. In vitro and in vivo studies on the degradation of high-purity Mg (99.99wt.%) screw with femoral intracondylar fractured rabbit model. Biomaterials 2015, 64, 57-69, DOI: 10.1016/j.biomaterials.2015.06.031.